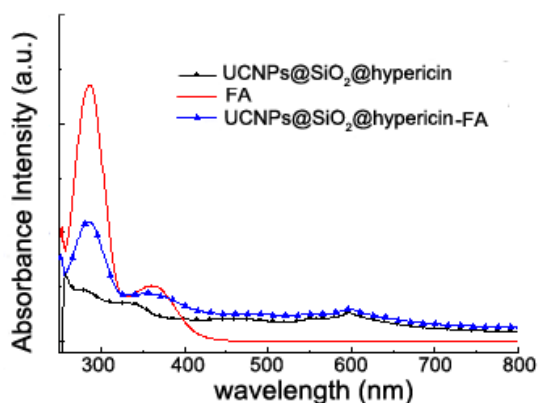


# 1 Multifunctional core-shell upconversion 2 nanoparticles for targeted tumor cells induced 3 by near-infrared light

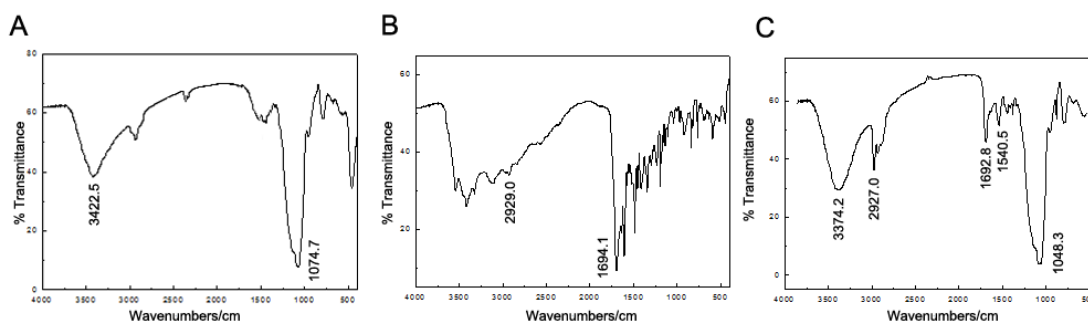
4 *Xiaojun Yang, Qianqian Xiao, Caixia Niu, Nan Jin, Jin Ouyang\*, Xueyuan Xiao\* and*  
5 *Dacheng He*

## 6 Supporting information



7  
8 **Fig.S1** UV/Vis absorption spectrum of UCNPs@SiO<sub>2</sub>@hypericin, FA,  
9 UCNPs@SiO<sub>2</sub>@hypericin-FA.

10  
11 As can be seen from Fig.S1, the UV/Vis absorption spectrum shows that FA has a  
12 strong peak at 280 nm. Meanwhile, the characteristic peak of FA appears in the  
13 UV/Vis absorption spectrum of UCNPs@SiO<sub>2</sub>@hypericin-FA compared with the  
14 UV/Vis absorption spectrum of UCNPs@SiO<sub>2</sub>@hypericin, which prove the success  
15 of the functionalization of the nanocomposites with FA.



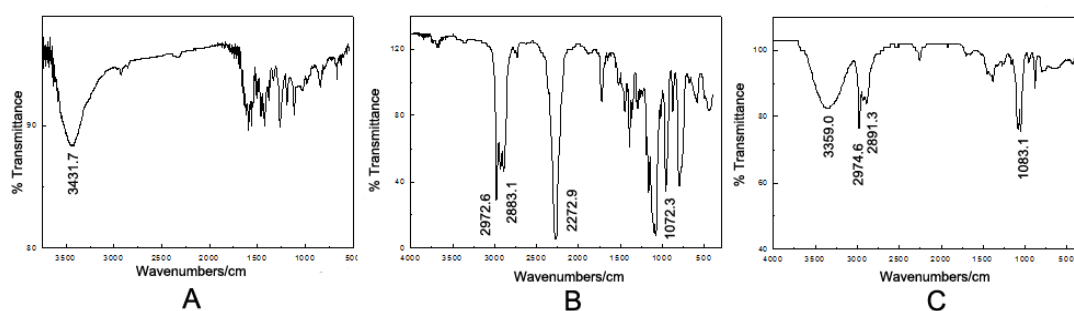
17

1 **Fig.S2** FTIR spectra of (A) UCNPs@SiO<sub>2</sub>@hypericin, (B) FA, and (C)  
2 UCNPs@SiO<sub>2</sub>@hypericin-FA.

3

4 The functionalization of the nanocomposites with folic acid was further investigated  
5 by FTIR shown in Fig. S2. In the FTIR spectrum of FA (Fig.S2B), a strong band at  
6 1694.1 cm<sup>-1</sup> was attributed to the C=O stretching vibrations of carboxyl group.  
7 Nevertheless, the feature above shrank remarkably after functionalization with FA,  
8 while a band at 1540.5 cm<sup>-1</sup> showed up, which was characteristic peak of the amido  
9 bond. Thus, successful functionalization of the nanocomposites with folic acid was  
10 confirmed based on the above.

11



12

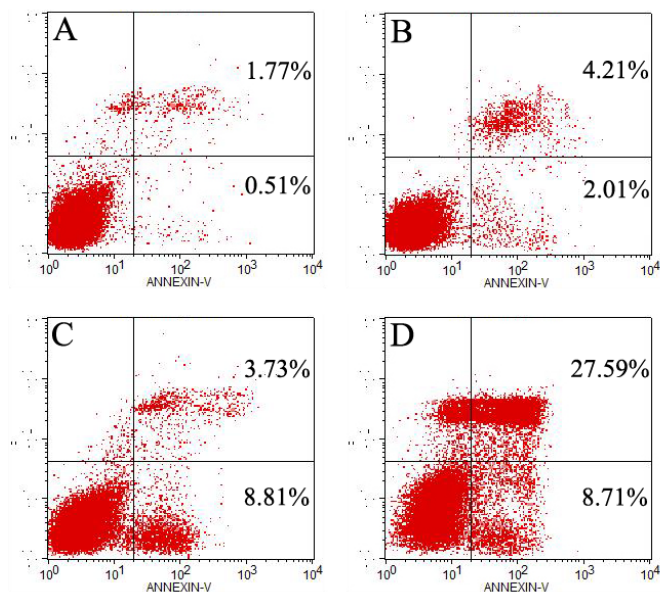
13 **Fig.S3** FTIR spectra of (A) hypericin, (B)TESPIC and (C)TESPIC-hypericin.

14

15 The formation of TESPIC-hypericin was investigated by FTIR shown in Fig.S3. In  
16 the FTIR spectrum of TESPIC(Fig.S3B), The transmission bands at 2272.9 cm<sup>-1</sup> were  
17 attributed to the -NCO stretching vibrations of isocyanate group. However, the  
18 characteristic peak almost disappeared in the FTIR spectrum of TESPIC-hypericin  
19 (Fig.S3C), which proved the successful synthesis of TESPIC-hypericin intermediates.

20

21 In this paper, loading rate is required by calculating the hypericin concentrations of  
22 solutions after the reaction under UV/Vis experiments. The input amount of hypericin  
23 in the synthesis of UCNPs@SiO<sub>2</sub>@hypericin-FA and UCNPs@SiO<sub>2</sub>(hypericin)-FA is  
24 the same and quantitative, so we can get the real loading rates. By the calculation, the  
25 loading rate of UCNPs@SiO<sub>2</sub>@hypericin-FA is 95.0% while the rate of  
26 UCNPs@SiO<sub>2</sub>(hypericin)-FA is 32.1%. As can be seen from the results, the amount  
27 of hypericin loaded in UCNPs@SiO<sub>2</sub>@hypericin-FA is higher. At the same time,  
28 references<sup>1-4</sup> have reported that organic reagents could easily combine with inorganic  
29 layer by covalent bonding with high efficiency.

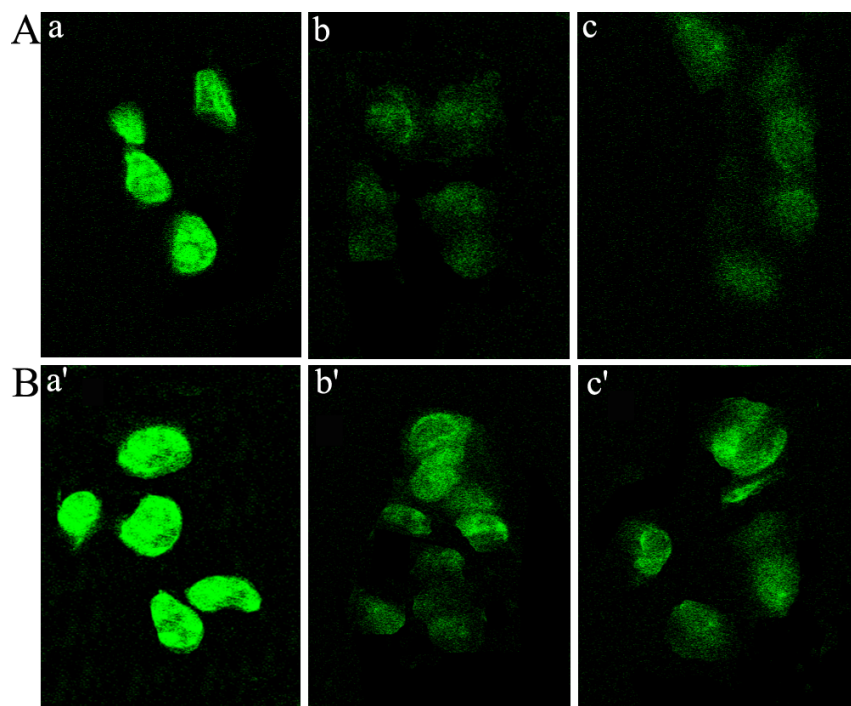


1

2 **Fig. S4** Flow cytometry of apoptosis of HeLa cells stained with Annexin V-FITC/PI induced by  
3 different loading rates of photosensitizer-bonded UCNPs@SiO<sub>2</sub>@hypericin-FA. The different  
4 loading rates are A) 19.6%, B) 38.2%, C) 63.1%, D) 95.0% respectively.

5

6 To prove the loading capacity affects the PDT efficiency, flow cytometry of apoptosis  
7 of HeLa cells induced by different loading rates of photosensitizer-bonded  
8 UCNPs@SiO<sub>2</sub>@hypericin-FA was carried on. The changes of apoptosis rate in the  
9 presence of different loading rates of photosensitizer-bonded  
10 UCNPs@SiO<sub>2</sub>@hypericin-FA were directly compared as shown in Fig.S4. The  
11 corresponding apoptosis rates were 2.28%, 6.22%, 12.54% and 36.30%, as expected,  
12 which indicated high loading rate of hypericin-bonded UCNPs@SiO<sub>2</sub>@hypericin-FA  
13 was more effective than the low loading rate of hypericin in the the PDT efficiency.



1

2 **Fig. S5** Confocal luminescence images of FR(+) HeLa cells and FR(-)293T cells incubated with  
3 UCNPs@SiO<sub>2</sub>@hypericin-FA or UCNPs@SiO<sub>2</sub>@hypericin under different concentrations, (A) 50  
4 µg·mL<sup>-1</sup>, (B) 200 µg·mL<sup>-1</sup>.

5 (a, a') FR(+) HeLa cells incubated with UCNPs@SiO<sub>2</sub>@hypericin-FA.

6 (b, b') FR(-)293T cells incubated with UCNPs@SiO<sub>2</sub>@hypericin-FA.

7 (c, c') FR(+) HeLa cells incubated with UCNPs@SiO<sub>2</sub>@hypericin.

8

9 The cell uptake studies were carried out under conditions of different concentrations  
10 of UCNPs@SiO<sub>2</sub>@hypericin-FA or UCNPs@SiO<sub>2</sub>@hypericin. As is shown in Fig.  
11 S5A, strong green upconversion luminescence was observed when HeLa cells were  
12 incubated with UCNPs@SiO<sub>2</sub>@hypericin-FA (Fig. 5S-a), however, there is much  
13 lower luminescence from 293T cells which were incubated with  
14 UCNPs@SiO<sub>2</sub>@hypericin-FA (Fig. 5S-b) and HeLa cells which were incubated with  
15 UCNPs@SiO<sub>2</sub>@hypericin (Fig. 5S-c). The same phenomenon appeared when the  
16 concentrations of UCNPs@SiO<sub>2</sub>@hypericin-FA or UCNPs@SiO<sub>2</sub>@hypericin were  
17 200 µg·mL<sup>-1</sup> (Fig. 5SB). All the above results showed that  
18 UCNPs@SiO<sub>2</sub>@hypericin-FA could selectively accumulate in the HeLa cells.

19

## 20 **References**

- 21 1 Li H.R., Lin J., Zhang H.J., Fu L.S., Novel covalently bonded hybrid materials of europium  
22 (terbium) complexes with silica. *Chem. Commun.*, 2001, **13**, 1212.  
23 2 Dong D.W., Jiang S.C., Men Y.F., Ji X.L., Jiang B.Z., Nanostructured hybrid organic-inorganic  
24 lanthanide complex films produced in situ via a sol-gel approach. *Adv. Mater.*, 2000, **12**, 646.

- 1 3 Franville A.C., Zambon D., Mahiou R., Luminescence behavior of sol–gel-derived hybrid  
2 materials resulting from covalent grafting of a chromophore unit to different organically  
3 modified alkoxy silanes. *Chem. Mater.* 2000, **12**, 428.
- 4 4 Hobson S.T., Shea K.J., Bridged Bisimide polysilsesquioxane xerogels: new hybrid  
5 organic–inorganic materials. *Chem Mater.*, 1997, **9**, 616